ISSN 2706-655X Vol.5, Issue 5: 48-56, DOI: 10.25236/IJFET.2023.050508

# Research on Structure Design and Simulation Test of Double-Layer Chain Plate Shared Dryer

**Lin Wei[1,a,*], Peng Guohua[1], He Zhibo[2], Chen Jing[3], Wang Chao[1], Chen Guihui[4], Wu Pan[1]**

*[1]School of Mechatronic Engineering, Southwest Petroleum University, Chengdu, 610500, China*
*[2]Yumen Drilling Branch of China Petroleum Corporation West Drilling Co. LTD, Jiuquan, 735008, China*
*[3]School of New Energy and Materials, Southwest Petroleum University, Chengdu, 610500, China*
*[4]School of Information Engineering, Southwest Petroleum University, Chengdu, 610500, China*
*[a]weilin_swpu@hotmail.com*
**Corresponding author*

***Abstract:*** *In order to reduce the fuel consumption rate of the traditional belt drying device and improve the utilization rate of the internal space of the drying equipment, a double-layer chain plate shared drying device is designed in this paper. The device adopts the chain plate transmission mode, which can simultaneously make use of the upper and lower chain plates of a transmission chain, and adopts the drying mode of combined heat source. Based on the gas-solid heat transfer theory, a numerical simulation model of the internal chamber of the dryer was established, and the temperature field variation of the hot air on the conveyor chain plate of the dryer was analyzed. Through numerical simulation analysis, the results show that the temperature field inside the oven is evenly distributed, and the temperature difference between the boundary and the internal temperature of the conveyor chain plate is small. Combined with the comparative analysis of chili drying process curve, it is verified that the drying device can effectively control the change of its internal temperature curve, and improve the drying efficiency and space utilization of the dryer. The research results of this paper will lay a theoretical foundation for the industrial application of the double-layer chain plate shared dryer.*

***Keywords:*** *Dryer. Chain plate, Combined heat source, Structural design, Coupling simulation*

## 1. Introduction

China is a largely agricultural country, and the harvest cycle of agricultural and sideline products is concentrated. An effective way to facilitate the preservation and transportation of agricultural products is drying, which is mainly to prevent the occurrence of microbial spoilage and mildew due to the high moisture content that accelerates the enzyme and metabolic activities in the product and the growth of microorganisms and bacteria[1-2]. The drying machine which can be used as large-scale drying agricultural products has been studied as an independent research field at home and abroad for decades. The time of domestic research on drying technology of agricultural products is short, which leads to the lack of planning for the development of drying technology as a whole. The existing drying equipment in China may have the following problems [3]: The drying object of many drying equipment is single, the automation and intelligence level of drying equipment is not high, the internal utilization rate of drying equipment is low, and the floor area is large. Many drying equipment uses electricity and coal as heat sources. Electricity as a heat source overloads the power grid load and is unbearable; coal has energy consumption, and high cost. Compared with domestic, western developed countries and emerging industrial areas of agricultural products the drying has been realized mechanization, drying equipment design and production is also increasingly perfect [4-5]. In addition, the research on drying methods abroad mainly focuses on the effects of hot air, microwave vacuum combination, and other advanced technologies on the quality of dried agricultural products [6-9].

According to the current situation of dryer in China and the international advanced technology, a double-layer chain plate shared drying device is designed in this paper. The use of double-layer chain plate can increase the space utilization rate, reduce the floor area, realize automatic control, and use the combined heat source with biomass as the main fuel to reduce the fuel consumption rate and reduce greenhouse gas emissions.

ISSN 2706-655X Vol.5, Issue 5: 48-56, DOI: 10.25236/IJFET.2023.050508

## 2. Structure Design and Working Principle of the Double-layer Chain Plate Shared Dryer

### *2.1. Overall structure design and working principle*

The drying device model for agricultural and sideline products is mainly composed of three systems, namely, drying system, material conveying system and air supply system. The main components are shown in Figure 1 Schematic diagram of agricultural by-products drying equipment.

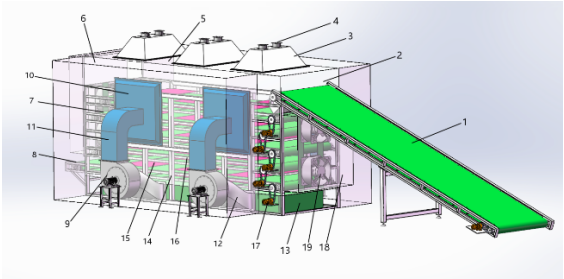

*1.material conveyor 2. material inlet 3. exhaust hood 4. ventilating fan 5. drying chamber 6. mounting chamber 7. chain plate conveyor 8. material outlet 9. centrifugal fan 10. hot air inlet 11. air outlet pipe 12. exhaust pipe 13. biomass combustion furnace 14. mounting frame 15. electric heating plate 16. infrared lamp tube 17. motor 18. mounting box 19. axial-flow fan*

*Figure 1: Schematic diagram of drying equipment for agricultural and sideline products*

The biomass combustion furnace is used as the main drying heat source, and the electric heating module and infrared lamp are used as auxiliary heating. In the combustion chamber, the air is heated by the heat generated by biomass combustion, and the air intake can be adjusted by adjusting the rotating speed of the centrifugal fan. By means of centrifugal fan, the hot air is sent into the drying chamber from the exhaust pipe through the air outlet pipe, and the agricultural products to be dried are sent into the chain plate conveyor from the material inlet through the conveyor. The agricultural products move from top to bottom with the chain plate conveyor, and the hot air is blown into the chain plate under the influence of four hot air outlets on the left and right. The chain plate is fixed with a turnover mechanism at each layer, and agricultural products will automatically fall off the lower layer of the chain plate under gravity when passing the turnover mechanism. For agricultural products in the effective drying area of the drying chamber, the speed of the motor is controlled by the control system according to the drying curve of different agricultural products, so as to control the drying time of agricultural products. When the agricultural products reach the outlet, the drying effect is achieved by gradually removing the moisture. The hot air flow can send the hot air to the combustion furnace through the air duct from the top exhaust port for secondary heating. The secondary heating air ensures that the desired temperature can be obtained efficiently. If the temperature on a certain layer fails to reach the pre-set temperature, the electric heating and infrared lamp heating uniformly distributed in the conveying mechanism can be turned on to ensure that the agricultural products reach its drying curve. The hot air path in the drying chamber is shown in Figure 2 Schematic diagram of hot air path.

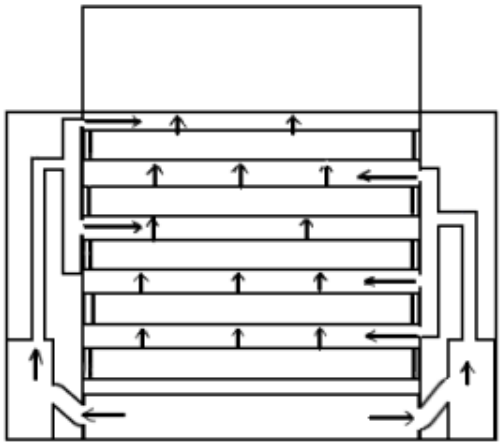

*Figure 2: Schematic diagram of hot air path*

ISSN 2706-655X Vol.5, Issue 5: 48-56, DOI: 10.25236/IJFET.2023.050508

### *2.2. Design of conveying mechanism*

The conveying mechanism of agricultural and sideline products is mainly used for feeding agricultural and sideline products to be dried and sending finished products after drying. The conveying mechanism is arranged in the drying chamber, so that the conveying mechanism is convenient for conveying the agricultural products in drying, and can also improve the drying time in the drying oven, thus ensuring the drying effect of agricultural and sideline products. The drying oven is provided with a mounting frame in the drying chamber, and the conveying mechanism includes four transmission chain plates, which are evenly interleaving distributed in the drying chamber from top to bottom. A conveyor is arranged at one side of the drying oven. When drying, agricultural and sideline products can be sent into the drying oven through the conveyor, and a guide plate is arranged at the end of the conveyor, which enables agricultural and sideline products to be transported to the top of the transmission chain plate; One side of the drying oven is provided with a delivery chain plate for collecting dried agricultural and sideline products.

The motor separately controls four transmission chain plates and the discharge transmission chain plates. The chosen material of the transmission shaft is 45 steel, and the material of the chain plate is 304 stainless steel mesh. Start the motor when the agricultural and sideline products are transported and dried. The output shaft of the motor rotates to drive the driving gear to rotate, and the driven gear meshing with the driving gear through the delivery chain can rotate under the drive of the driving gear. The transmission shaft can rotate under the drive of the driven gear, and then the delivery chain meshing with the transmission gear set on the driven gear can rotate under the drive of the transmission gear, so as to drive the chain plate to operate, thus facilitating the transportation of agricultural and sideline products. The speed of each layer is independent, controllable and adjustable, and the transportation time of agricultural and sideline products in the dryer can be independently controlled by the control system.

### *2.3. Turnover mechanism*

The turnover mechanism is in the conveying mechanism, and its main function is to prolong the drying time of agricultural and sideline products in the drying oven. It makes the drying capacity and drying time of the dryer for agricultural and sideline products at least twice higher than that of traditional belt dryer with the same volume.

The delivery chain far from the motor is provided with a connecting plate connected with the connecting shaft, and the end of the connecting plate is provided with a long shaft and a short shaft. The frame is provided with a turnover plate close to the connecting plate, and the turnover plate is provided with a limit groove suitable for the long shaft and the short shaft. When the motor drives the chain plate to transport agricultural and sideline products, the limit groove can limit the long shaft and short shaft, which can enable the chain plate to transport agricultural and sideline products smoothly. The Single-chain plate is shown in Figure 3.

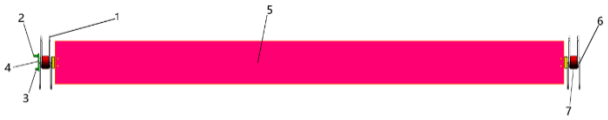


*1. chain 2. long shaft 3. short shaft 4. connecting plate 5. chain plate 6. single shaft 7. chain wheel*

*Figure 3: Single-chain plate structure*

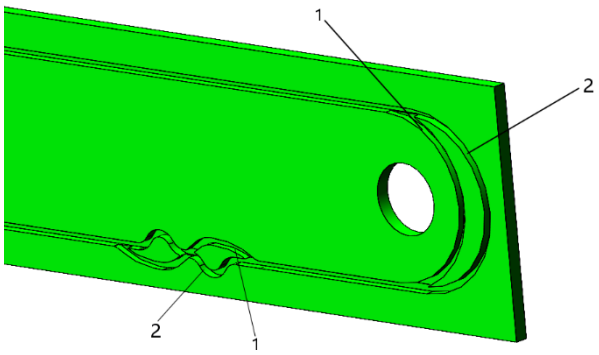


*1. deep groove 2. shallow groove*

*Figure 4: Schematic diagram of limit groove of turnover plate*

ISSN 2706-655X Vol.5, Issue 5: 48-56, DOI: 10.25236/IJFET.2023.050508

One end of the turnover plate is provided with a turnover groove which is connected with the limit groove. The turnover groove is in the shape of "8", which includes a deep groove and a shallow groove. When the chain plate passes through the turnover groove, the long shaft can pass through the deep groove, and the short shaft can pass through the shallow groove, and then can realize the 180 ° turnover of the chain plate, so that all the agricultural and sideline products on the upper chain plate can fall onto the lower chain plate. The problem that agricultural and sideline products with smaller particles are stuck in the gap between two adjacent chain plates is reduced. The turnover plate is shown in Figure 4.

## 3. Numerical simulation analysis and verification of dryer

For verification data, the paper adopted the hot-air drying test of chili on the thin-layer drying test bed that is conducted by Gao Guohua [10]. He selected the hot air temperature and wind speed as test factors, and made several sets of experimental research between hot-air drying of chili under constant temperature drying and that under controlled temperature by stages. Under the hot-air drying of constant temperature condition and that of controlled temperature by stages, the better comprehensive scores of chili are not much different. The range of influence factors under the better conditions preliminarily judged is also similar, that is, the hot-air temperature is between 55℃ and 65℃, more close to 55 ℃, the wind speed is about 1.2m/s on the left, and the drying time is between 300 minutes and 450 minutes.

### *3.1. Gas-solid-thermal coupling numerical simulation modeling*

According to the established drying device model, the temperature field in the drying oven is mainly modeled and analyzed. The numerical simulation models of four delivery chains and eight chain plates are established. As shown in Figure 5.

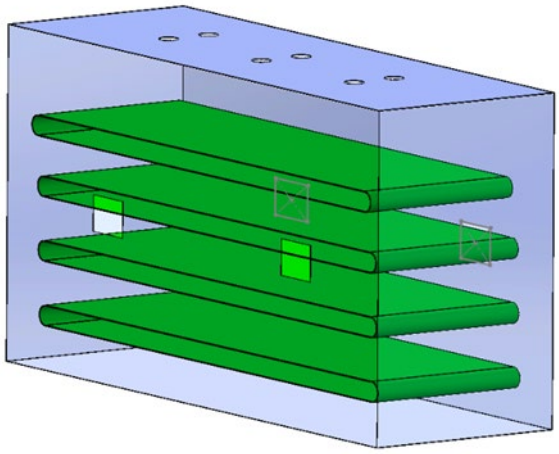

*Figure 5: Establishment of drying oven model*

According to the established three-dimensional solid model, the finite element simulation model as shown in Figure 6 is built by using the finite element simulation method. The whole computing domain has 1.94 million units.

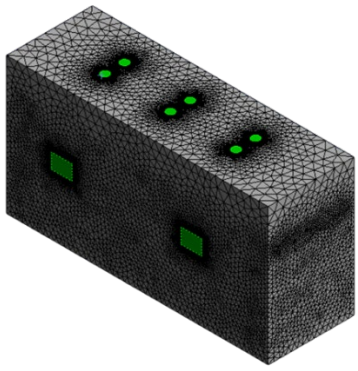

*Figure 6: Grid division model*

ISSN 2706-655X Vol.5, Issue 5: 48-56, DOI: 10.25236/IJFET.2023.050508

The drying medium inside the dryer is hot air, which is discharged by the axial-flow fan, blown into the drying chamber, and dispersed by the axial-flow fan to make it evenly distributed. Therefore, the air flow state is very complex, and it is unsteady turbulent flow. Therefore, when selecting the computational model for simulation, Realizable k-ε model with good convergence performance and reasonable accuracy is selected. When selecting the wall function, in order to prevent the simulated fluid from distortion when flowing on the wall, the standard wall function is selected, which is more similar with the gas flow inside the dryer. In Realizable k-ε model, turbulent kinetic energy equation k and turbulent dissipation equation [11] are respectively ε:

$$\rho\frac{dk}{dt}=\frac{\partial}{\partial xi}\left[\left(\mu+\frac{\mu_t}{\sigma_k}\right)\frac{\partial k}{\partial xi}\right]+G_k+G_b-\rho\varepsilon-Y_M \tag{1}$$

$$\rho\frac{d\varepsilon}{dt}=\frac{\partial}{\partial xi}\left[\left(\mu+\frac{\mu t}{\sigma_\varepsilon}\right)\frac{\partial_\varepsilon}{\partial xi}\right]+\rho C_1 S\varepsilon-\rho C_2\frac{\varepsilon^2}{k+\sqrt{\upsilon\varepsilon}}+C_{1\varepsilon}\frac{\varepsilon}{k}C_{3\varepsilon}G_b \tag{2}$$

where $C_1=\max\left(0.43,\frac{\eta}{\eta+5}\right),\eta=Sk/\varepsilon$.

In the above equation, $G_k$ represents the generation of turbulent kinetic energy due to the average velocity gradient, and $G_b$ represents the generation of turbulent kinetic energy due to buoyancy; $Y_M$ is the influence of compressible turbulent fluctuation expansion on the total dissipation rate; $C_2$ and $C_{1\varepsilon}$ are constants; $\sigma_k$ and $\sigma_\varepsilon$ are turbulent Prandtl numbers of turbulent kinetic energy and its dissipation rate respectively. In Fluent, as the default constants, $C_{1\varepsilon}$ =1.44, $C_2$=1.9, $\sigma_k$ =1.0, $\sigma_\varepsilon$ =1.2.

In the process of numerical calculation with air as the flowing medium, density ρ=1.000 kg/m3, and viscosity μ=2.11×10-5 Pa·S. Chain plate is made of 304 stainless steel. Density (20℃, g/cm³) is 7.93, and specific heat capacity (0~100℃, KJ·kg-1K-1) is 0.50. When the temperature is 100℃, the thermal conductivity (W·m-1·K-1) is 16.3. When the temperature is 500℃, the thermal conductivity (W·m-1·K-1) is 21.5.

The setting of boundary conditions and specific parameters are as above. Monitoring is set in each layer of chain plate and the whole chain plate in the dryer computing domain to detect the temperature change of each layer of plate.

### *3.2. Analysis of simulation results*

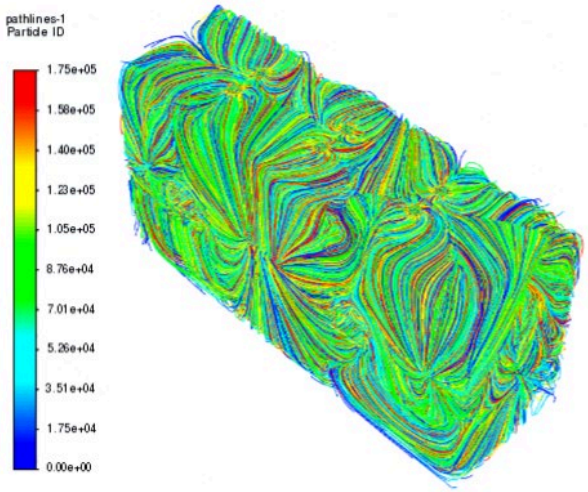


*Figure 7: Streamline chart inside the drying oven*

ISSN 2706-655X Vol.5, Issue 5: 48-56, DOI: 10.25236/IJFET.2023.050508

The flow path of the internal air flow of the dryer can be represented by a streamline chart. The simulation results of the internal air flow are shown in Figure 7. The hot air is blown in from the hot air inlet. First, it blows to the upper two layers of the chain plate, passes through the chain plate and circulates downward, and finally fills the entire drying oven.

The main parameters set at the inlet are as follows: temperature is 65℃, initial temperature is 35℃, and wind speed is 1.2m/s. The temperature nephogram of all chain plates after calculation and the comparison nephogram of each layer of the chain plate are shown in the following figure 8.

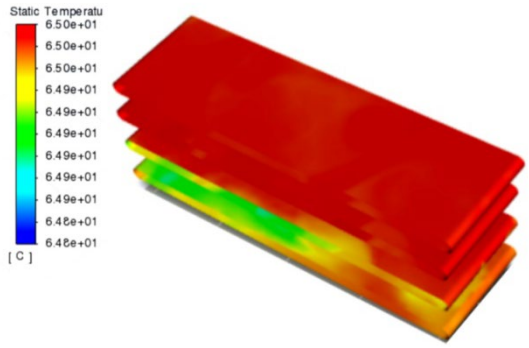


*Figure 8: Temperature distribution nephogram of all chain plates*

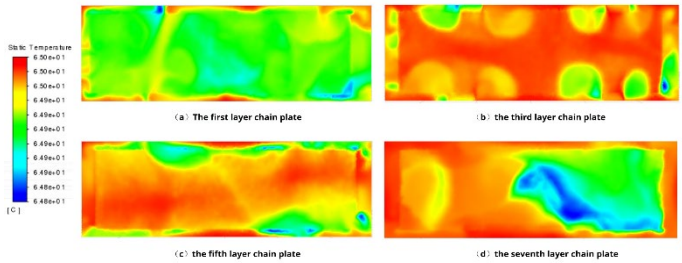


*Figure 9: Temperature distribution nephogram of first, third, fifth, and seventh layer*

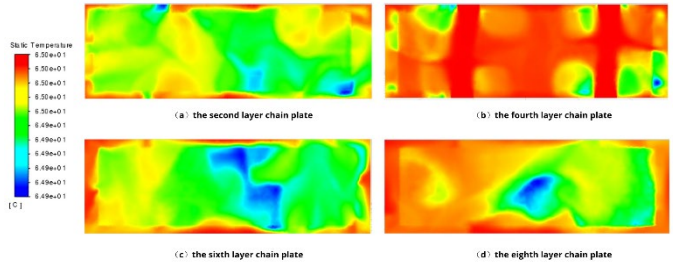


*Figure 10: Temperature distribution nephogram of second, fourth, sixth, and eighth layer*

It is found from the temperature distribution nephogram fig.9 and 10 that: first, under the set temperature and speed, each layer of chain plate can reach the expected temperature, and the temperature difference can be controlled within 0.5℃, indicating that the device can meet the expected effect in structure. Second, by analyzing the temperature nephogram of the odd-layer and even-layer chain plates, the chain plate near the air inlet first reaches the predetermined temperature, and the chain plate far away from the air inlet reaches the predetermined temperature last, indicating that the crops at the chain plate near the air inlet are subjected to high temperature gas for a long time, thus resulting in burning, which needs to be optimized later.

### *3.3. Analysis of space utilization and energy consumption*

The interior of the belt dryer is mainly composed of the conveying space that is composed of conveyor, cavity and unavailable space. The conveying space is used for the flow of high-temperature gas, and the unavailable space is used for installing related instruments, such as frame, pipe, and auxiliary equipment. The definition of each space is as follows:

ISSN 2706-655X Vol.5, Issue 5: 48-56, DOI: 10.25236/IJFET.2023.050508

Definition 1: Effective conveying space S= (S1, S2, S3…Sn), where Sn is the effective single-layer conveying space that can be directly calculated, and n refers to the number of belt layers inside the belt dryer.

Definition 2: Cavity=Y, Y is the effective flow space of high-temperature gas in the dryer that can be directly calculated.

Definition 3: Unavailable space is W, which refers to the space occupied by all frames, pipes, conveyors, and auxiliary equipment that cannot be used.

Definition 4: V=S+Y+W, where V is the volume of the dryer.

According to the above definitions, the evaluation formula of space utilization inside the dryer can be established as follows:

$$\sigma = \frac{V_0}{V} \times 100\% \tag{3}$$

where A is the space utilization rate, which refers to the proportion of effective conveying space in the dryer and is used to measure the space utilization rate of the dryer.

The effective conveying space is S, cavity is Y, and unavailable space is W, and they are all determined by the design scheme. So equation (3) can be transformed to:

$$\sigma = \frac{V - Y - W}{V} \times 100\% \tag{4}$$

The internal flow chart (left) of the traditional multi-layer belt dryer [12] and the internal flow chart (right) of the double-layer chain plate shared dryer designed in this paper are as follows:

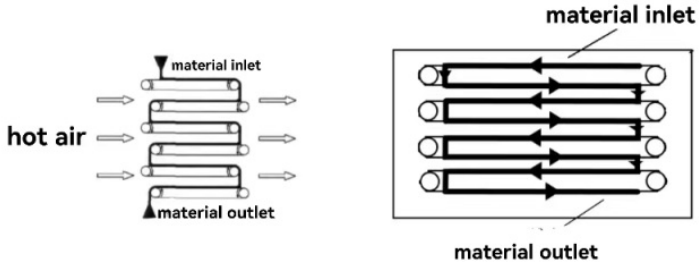


*Figure 11: Internal flow chart of traditional multi-layer belt dryer and double-layer chain plate shared dryer*

By comparing the two flow charts in Figure 11, the double chain plate shared dryer designed in this paper can use the transmission part that even layers of the multi-layer belt dryer cannot use. In the case of the same volume, the double-layer chain plate sharing type dryer designed in this paper is twice as efficient as the multi-layer belt dryer; If the working efficiency is the same, the volume of the double-layer chain plate shared dryer designed in this paper is at least half that of the multi-layer belt dryer.

According to the model, Y≈25m, W≈5m and S≈10m of the double-layer chain plate shared dryer in the paper are measured. According to equation (4), the space utilization rate δ of the double-layer chain plate shared dryer is about 25%. Under the same conditions, the space utilization rate of multi-layer belt dryer is only 12.5%.

It can be concluded that the double-layer chain plate dryer designed in this paper can greatly improve the space utilization rate, and can greatly reduce the volume of the dryer under the same drying efficiency. This design solves the problem that the traditional belt dryer occupies a large space with low utilization rate and improves the utilization rate of energy.

Energy consumption refers to the consumption of energy resources. The double-layer chain plate shared dryer designed in this paper uses biomass as the main energy and electricity as the auxiliary energy to generate heat. Traditional continuous dryers mainly use coal-fired hot-blast stove as the main heat source [13]. In the energy-saving and economic analysis on CPH system of biomass direct combustion power generation studied by Qu Lei and Li Hua [14], the biomass burned in the project reached 95976t/a, which is equivalent to about 35352t/a of standard coal when calculated by 29270kJ/kg of low calorific value of standard coal. If biomass is burned instead of coal, about 35352t/a standard coal can be saved

ISSN 2706-655X Vol.5, Issue 5: 48-56, DOI: 10.25236/IJFET.2023.050508

every year. It can be seen that using biomass as fuel can significantly reduce energy consumption.

### *3.4. Comparative study on drying process curves of chili*

With chili as the simulation research object, the drying rate refers to the loss of moisture mass of fresh chili per unit time [15], which can be expressed by the formula:

$$V = \frac{G_2}{T} \tag{5}$$

$$G_2 = G_1 - G_t \tag{6}$$

where V is the drying rate (g/min); $G_1$ is the mass of fresh chili in each test (g); $G_t$ is the amount of dry matter of chili after each test (g); T is the drying time of each test (min).

$G_1$ and $G_t$ of each test are fixed, so the drying rate of chili can be measured by the time taken for each drying. According to Gao Guohua, Chen Jian [16] et al., the drying rate curves of chili under the same wind speed and different temperatures obtained in the Experiment and Research between Hot-air Drying of Chili under Constant Temperature and that under Controlled Temperature by Stages are taken as the reference objects.

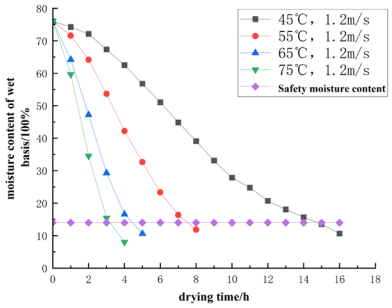


*Figure 12: Drying rate at different temperatures with wind speed of 1.2m/s*

The single-layer conveying chain plate of the double-layer chain plate shared dryer designed in this paper is 6.3m long, 1.7m wide, and its actual working length is 50.4m. Each layer is loaded with 4cm, which can simultaneously load crops with a volume of 3.4m$^3$.

Each layer of the chain plate conveyor is controlled by the motor separately. When the same raw materials are used, the control motor only needs to make the time from the material inlet to the material outlet controlled within 3hours to 8hours to complete the drying of chili, an agricultural product.

Simple calculation is carried out by the speed time formula:

$$V_1 = \frac{S_1}{T_1} \tag{7}$$

where $V_1$ is the transmission rate of the chain plate, $S_1$ is the distance of the chili in the dryer, and $T_1$ is the reference time.

According to the calculation result, the chain plate moving rate is controlled at the speed of 0-0.21m/min in theory, which can meet the drying requirements of chili, that is, the above curve fig.12 is met. Therefore, the double-layer chain plate shared dryer designed in this paper can theoretically meet the drying task of chili in theory.

## 4. Conclusion

In the paper, a double-layer chain plate shared drying device is designed. Based on the gas-solid-thermal coupling theory, the temperature field variation rule of hot air on the conveying chain plate of the dryer is analyzed. Combined with the comparison and analysis of the drying process curve of chili, the following conclusions are drawn:

ISSN 2706-655X Vol.5, Issue 5: 48-56, DOI: 10.25236/IJFET.2023.050508

(1) A double-layer chain plate shared dryer is proposed in the paper, which can simultaneously make use of the upper and lower layers of chain plates of a transmission. In this way, it increases the space utilization rate, reduces floor area, realizes automation, reduce fuel consumption and environmental pollution, etc.

(2) Through the simulation analysis of gas-solid-thermal coupling inside the dryer, it is obtained that the temperature on the chain plates of each layer is basically evenly distributed, which verifies that the dryer can effectively control the temperature inside the oven.

(3) Through the comparative study of chili processing curves, it is verified that the dryer has high space utilization rate and low energy consumption.

## Acknowledgments

The authors express their appreciation to Nanchong City-SWPU Science and Technology Strategic Cooperation Project (Grant No. SXJBGS003, SXHZ022, SXHZ023, SXQHJH058).

## References

*[1] Maganioti A E, Chrissanthi H D, Charalabos P C, et al. Cointegration of event-related potential (ERP) signals in experiments with different electromagnetic field (EMF) conditions [J]. Health, 2010, 2(05): 400.*

*[2] Bootorabi F, Haapasalo J, Smith E, et al. Carbonic anhydrase VII–a potential prognostic marker in gliomas [J]. Health, 2011, 3(01): 6.*

*[3] Süfer Ö, Palazoğlu TK. A study on hot-air drying of pomegranate: kinetic of dehydration, rehydration and efects on bioactive compounds. J Therm Anal Calorim. 2019; 137:1981–90.*

*[4] Selimefendigil F, Çoban SÖ, Öztop HF. Convective drying of a moist porous object under the efects of a rotating cylinder in a channel. J Therm Anal Calorim. 2019. https://doi. org/10. 1007/ s10973-019-09140-5.*

*[5] Hu Bin. Design and Research of Continuous Dryer [D]. Anhui Agricultural University, 2013.*

*[6] A. Balasubramanian, Panda, Ramachandra Rao. Modeling a fluidized bed dryer usingartificial neural network [J]. Drying Technology, 2003, (14):7-8.*

*[7] Gheorghita Jinescu, V. Lavric. The artificial neural network and the drying processmodeling [J]. Drying Technology, 2006, (13):5-7.*

*[8] Oberoi HS, Ku MA, Kaur J. Quality of red chilli variety as af- fected by different drying methods[J]. Journal of food sci- ence and Technology-mysore, 2005, 42(5): 384-387.*

*[9] Ibrahim Doymaz, Mehmet Pala. Hot-air drying characteristics of red pepper [J]. Journal of Food Engineering, 2002, 55 (4): 331-335.*

*[10] Kaensup W, Chutima S, Wongwises S. Experimental study on drying of chilli in a combined microwave - vacuum-rotary drum dryer [J]. Drying Technology, 2002, 20 (10): 2067 -2079.*

*[11] T. Y. Tunde-Akintunde. Mathematical modeling of sun and solar drying of chilli pepper [J]. Renewable Energy, 2011, 36(8).*

*[12] Gao Guohua. Contrast between Hot-air Drying of Chili under Constant Temperature and that under Graded and Controlled temperature [D]. Southwest University, 2012.*

*[13] Zhang Chengcheng, Fu Weiliang, Huang Jiazhen, Zhang Xukun. Optimization Design of Mesh Belt Dryer based on CFD [J]. Guangdong Chemical Industry, 2022, 49(18): 157-160.*

*[14] Chang Jian, You Changjing, Yang Deyong, Liu Xiangdong. Optimization of Drying Process for Multilayer Belt Dryer [J]. Transactions of the Chinese Society for Agricultural Machinery, 2012, 43(08):148-154.*

*[15] Luo Dong, Sun Huinan, Xia Chaoyong. The Development Status of Counter-concurrent Flow Continuous Dryer in China [J]. Modern Food, 2021(08): 23-24+29.*

*[16] Qu Lei, Li Hua. The Energy-Saving and Economic Analysis on CHP System of 12MW Biomass Direct Combustion Power Generation [J]. Energy research and Utilization, 2010(02):37-39.*

*[17] Zheng Yan, Chen Jian, Xie Shouyong, Zhao Chao. Contrast between Heated Air Drying of Chinese Prickly Ash under Constant Temperature and that under Graded and Controlled Temperature [J]. Transactions of the Chinese Society of Agricultural Engineering, 2008(02):277-280.*

*[18] Gao Guohua, Chen Jian, Li Yunwu, Guo Shun. Experiment and Research between Hot-air Drying of Chili under Constant Temperature and that under Controlled Temperature by Stages [J]. Journal of Agricultural Mechanization Research, 2012, 34(09):159-163.*